Kybernetika

Muhammad Idrees; Shah Muhammad; Saif Ullah

Robust hierarchical sliding mode control with state-dependent switching gain for stabilization of rotary inverted pendulum

ROBUST HIERARCHICAL SLIDING MODE CONTROL WITH STATE-DEPENDENT SWITCHING GAIN FOR STABILIZATION OF ROTARY INVERTED PENDULUM

Muhammad Idrees, Shah Muhammad and Saif Ullah

The rotary inverted pendulum (RIP) system is one of the fundamental, nonlinear, unstable and interesting benchmark systems in the field of control theory. In this paper, two nonlinear control strategies, namely hierarchical sliding mode control (HSMC) and decoupled sliding mode control (DSMC), are discussed to address the stabilization problem of the RIP system. We introduced HSMC with state-dependent switching gain for stabilization of the RIP system. Numerical simulations are performed to analyze the performance of the hierarchical sliding mode controllers with the decoupled sliding mode controller and the controller obtained from the pole placement technique. We proposed HSMC with state-dependent switching gain as it shows better performance as compared to HSMC with constant switching gain, DSMC, and the state feedback controller based on pole placement technique. The stability analysis of proposed HSMC is also discussed by using Lyapunov stability theory.

Keywords: rotary inverted pendulum, sliding mode control, dynamical systems

Classification: 93A30, 93C10, 93D05, 93D09, 93D20

1. INTRODUCTION

Sliding mode control (SMC) due to its simplicity of design has been successfully employed for solving nonlinear control problems [12, 15, 16, 20]. It was first used in the 1960s and its basic formulations are due to the work of Utkin [44]. Utkin provided the definition of the sliding surface from which equivalent control is derived. Utkin together with Yang continued their work and in 1978, they derived the term nonlinear switching from linear state space derivation which ensured the robustness of SMC [45]. Based on SMC, different new techniques are designed to address nonlinear control problems [36, 41, 48, 53]. It is widely used to design controllers for robotics [33, 37, 54], under-actuated cranes [21, 27, 42, 43], quadrotors for unmanned aerial vehicles (UAV) [1], and under-actuated vessels [22].

The main features of SMC include robustness, easy tuning, and implementation [2, 8]. It uses Lyapunov function to guarantee the robustness property which makes SMC a better option as compared with other control design techniques. However, a known drawback of this nonlinear control technique is chattering. To overcome this problem, Slotine

proposed adopting thin boundary layer neighboring switching surfaces, by replacing the sign function with a saturation function [38].

Inverted pendulum (IP) systems represent a significant class of nonlinear underactuated mechanical systems, well-suited benchmarks for the validation and practical application of ideas emerging in control theory and robotics. The RIP system is an example of IP systems that have numerous real-life applications, for example, control of satellite and aerospace vehicles [9, 30], and balancing robots [24, 25]. Stabilization of a pendulum rod in the unstable upright position is considered a benchmark control problem that has been solved by attaching the pendulum to a base that rotates in a horizontal plane [3, 13].

This article is concerned with the RIP system which consists of an inverted pendulum in a plane perpendicular to the rotating arm. Various control methodologies for the RIP systems have been proposed. Jinquan presented a model analysis control algorithm based on the state feedback method. Irfan et al also proposed a control design algorithm based on the state feedback method for controlling the RIP [11]. Hassanzadeh designed a controller for the RIP system using evolutionary algorithms [10]. Jose used (Proportional-Integral-Derivative) PID and (Linear Quadratic Regulator) LQR control techniques to balance the pendulum in its upright position [14]. Kurode used sliding modes for the swing-up and stabilization of the RIP [17]. Yigit used a model-free sliding mode approach to stabilize the RIP system [51] and Zhang used nonlinear SMC to stabilize the RIP while a fuzzy-PD regulator was applied to stabilize the rotary pendulum by Oltean [29]. Khanesar proposed fuzzy sliding mode control for the stabilization of the RIP systems [18].

In addition, many advanced control techniques are also used to stabilize the RIP system: for examples, Chen used adaptive control [4], Sirisha used H_∞ control [39], Wu et. al. used the Lagrange modeling method [49], and Yue et. al. used an indirect adaptive fuzzy control technique [52]. All these control techniques are used to achieve the same objective. Some of the control techniques described above are using linearization of the mathematical model of the RIP system around an unstable equilibrium point. If the pendulum is far from that point, then these control techniques do not give satisfactory results. Some control structures do not consider the stability while others are overly intricate. Many of these control techniques did not consider robustness. Recently, Wen designed a controller for stabilizing the RIP system based on a logarithmic Lyapunov function [50]. His simulation results are satisfactory. However, he used the linearized model of the RIP system that may not reflect the performance of controller completely because the RIP is a highly nonlinear system.

Among the possible robust control strategies, SMC attributes such as low complexity, low computational burden, less weight and low-cost control method make this a suitable approach to be implemented for stabilization of the RIP system [32]. Further, the mathematical model of the RIP systems is strongly nonlinear single-input and multi-output system. Therefore, in this paper, we introduced two up-gradations of the SMC to address the stabilization problem of the RIP system. The aim is to determine which one is the better one.

The main goal of this article is to provide an appropriate nonlinear control methodology for the RIP system that is intrinsically nonlinear. The main contribution of this

paper is to analyse and investigate the more suitable hierarchical sliding mode controller for the RIP systems. We design both hierarchical and decoupled sliding mode control for stabilization of the RIP systems and both give better performance as compared to other complicated control techniques.

The remainder of this paper is organized as follows. In the second section of this article, mathematical model of the RIP system is presented. In the third section, complete description of HSMC is provided while in the fourth section, description of DSMC is discussed. In the fifth section, stability analysis of HSMC is discussed. In the sixth section, results of numerical simulations are presented. The conclusion of the article is given in the seventh section, followed by a statement acknowledgement and the list of references.

2. MATHEMATICAL MODEL OF THE ROTARY INVERTED PENDULUM

In 1992, the RIP system was first introduced by Furuta [7]. Since then, the RIP system has also been known as the Furuta pendulum. The structure of the RIP system is described in Figure 1. It consists of a pendulum of length L attached to a rotating horizontal bar of length r. The pendulum sets up an angle α in the vertical direction, and the horizontal bar moves in clockwise and anticlockwise directions with an angle θ. The motion of the pendulum is in the vertical plane, while rotation of horizontal bar is in the horizontal plane.

The mathematical model of the RIP system consists of two second-order nonlinear differential equations given below [19]:

$$\varsigma_1\ddot{\theta} - (\varsigma_2\cos\alpha)\ddot{\alpha} + \varsigma_2\sin\alpha(\dot{\alpha})^2 + \varsigma_5\dot{\theta} = \varsigma_6 V_m \ , \tag{1}$$

$$\varsigma_3\ddot{\alpha} - (\varsigma_2\cos\alpha)\ddot{\theta} - \varsigma_4\sin\alpha = 0 \ , \tag{2}$$

where $\varsigma_1 = J_{\mathrm{eq}} + mr^2$, $\varsigma_2 = mLr$, $\varsigma_3 = \frac{4}{3}mL^2$, $\varsigma_4 = mgL$, $\varsigma_5 = \frac{\eta_m\eta_g K_t K_m K_g^2 + B_{\mathrm{eq}}R_m}{R_m}$, and $\varsigma_6 = \frac{K_t K_g \eta_m \eta_g}{R_m}$. The description of the parameters of this model is given in Table 1. The state space representation of the RIP system is:

$$\left.\begin{aligned}
\dot{x}_1 &= x_2 \, , \\
\dot{x}_2 &= f_1(x) + b_1(x)\tau + \Delta \, , \\
\dot{x}_3 &= x_4 \, , \\
\dot{x}_4 &= f_2(x) + b_2(x)\tau + \Delta \, ,
\end{aligned}\right\} \tag{3}$$

where x_1 represents angle of inverted pendulum, x_2 represents angular velocity of inverted pendulum, x_3 represents angle of horizontal bar, x_4 represents angular velocity of horizontal bar, τ represents control input, and Δ is bounded external disturbance.

Symbol	Description
m	Mass of Pendulum
g	Gravitational Acceleration
η_m	Motor Efficiency due to Rotational Loss
η_g	Gearbox Efficiency
K_t	Motor Torque Constant
K_m	Back EMF Constant
K_g	Rotary Servo Base Unit (SRV02) Gear Ratio
R_m	Armature Resistance
V_m	Input Voltage
B_{eq}	Equivalent Viscous Friction

Tab. 1. Description of parameters of the RIP system.

The nonlinear functions f_1, f_2, b_1 and b_2 of state variables are given below:

$$f_1(x) = \frac{-\frac{\varsigma_2^2}{2}\sin(2x_1)x_2^2 - \Gamma_2\varsigma_5 x_4 + \varsigma_1\Gamma_3}{\Gamma_1 - \Gamma_2^2},$$

$$f_2(x) = \frac{\varsigma_3 f_1(x) - \Gamma_3}{\Gamma_2},$$

$$b_1(x) = \frac{\Gamma_2\varsigma_6}{\Gamma_1 - \Gamma_2^2},$$

$$b_2(x) = \frac{\varsigma_3\varsigma_6}{\Gamma_1 - \Gamma_2^2},$$

where $\Gamma_1 = \varsigma_1\varsigma_3$, $\Gamma_2 = \varsigma_2 \cos x_1$, and $\Gamma_3 = \varsigma_4 \sin x_1$. The RIP system have two equilibrium points which are $(0, 0, 0, 0)$ and $(\pi, 0, 0, 0)$. The point $(\pi, 0, 0, 0)$ is stable but $(0, 0, 0, 0)$ is unstable. The control objective is to smoothly stabilize the pendulum at the unstable equilibrium point $(0, 0, 0, 0)$ in a short time in the presence of bounded external disturbances.

3. HIERARCHICAL SLIDING MODE CONTROL

Sliding Mode Control (SMC) is constructed to drive the system states onto a particular surface in the state space. This surface is called the sliding surface. Once the sliding surface is reached, SMC keeps the system states in the close neighborhood of the sliding surface [31, 46, 47]. Hence the sliding mode control design technique consists of two parts. In the first part, we design a sliding surface so that the sliding motion satisfies design specifications. The second part is concerned with the selection of a control law that will make the sliding surface attractive for the system states. Therefore, SMC
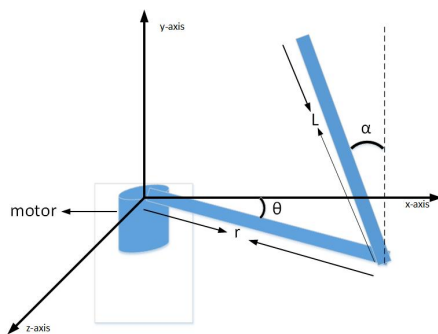
Fig. 1. Structure of the rotary inverted pendulum.

consists of an equivalent control and a switching control. i. e.,

$$\tau = \tau_{\text{eq}} + \tau_{\text{sw}} . \tag{4}$$

Several control techniques and applications in the fields of sliding mode control for the RIP system have been published in various journals and conference proceedings [5, 18, 19, 51]. In spite of all these advances, still there is need to work more in this field. HSMC is the systematic and effective design procedure, which has both theoretical and practical significance [32]. It fills the gap between sliding mode control and its applications to the RIP system. HSMC is a technique which consists of two types of sliding surfaces which are called the first-level sliding surface and the second-level sliding surface [34, 35].

To design HSMC for the RIP system, we divide the given system into two subsystems. Subsystem I includes the state variables x_1 and x_2, while the subsystem II includes the state variables x_3 and x_4. HSMC for the given system consists of two first-level sliding surfaces and one second-level sliding surface. The structure of hierarchical sliding mode surfaces is illustrated in Figure 1.

We define the 1st first-level sliding surface as:

$$\sigma_1 = \varrho_1 x_1 + x_2 , \tag{5}$$

where ϱ_1 is a positive constant. Differentiating Eq.(5) w.r.t 't', we have

$$\dot{\sigma}_1 = \varrho_1 \dot{x}_1 + \dot{x}_2 , \tag{6}$$
$$\dot{\sigma}_1 = \varrho_1 x_2 + f_1(x) + b_1(x)\tau + \Delta . \tag{7}$$

Let $\dot{\sigma}_1 = 0$, the equivalent control of subsystem I is obtained as:

$$\tau_{\text{eq1}} = -\frac{\varrho_1 x_2 + f_1(x) + \Delta}{\mid b_1(x) \mid + \delta} , \tag{8}$$

where δ is a small positive constant to avoid indeterminate form when $b_1(x)$ is zero. As δ is positive, so we are also using here absolute value of $b_1(x)$ to avoid zero in the

denominator when $\mid b_1(x) \mid +\delta$ is zero. We define the 2nd first-level sliding surface as:

$$\sigma_2 = \varrho_2 x_3 + x_4 \ , \tag{9}$$

where ϱ_2 is a positive constant. Differentiating Eq.(9) with respect to time 't', we have

$$\dot{\sigma}_2 = \varrho_2 \dot{x}_3 + \dot{x}_4 \ , \tag{10}$$

$$\dot{\sigma}_2 = \varrho_2 x_4 + f_2(x) + b_2(x)\tau + \Delta \ . \tag{11}$$

Let $\dot{\sigma}_2 = 0$, the equivalent control of subsystem II is obtained as:

$$\tau_{\mathrm{eq2}} = -\frac{\varrho_2 x_4 + f_2(x) + \Delta}{\mid b_2(x) \mid +\delta} \ . \tag{12}$$

We define the second-level sliding surface as a linear combination of both the first-level sliding surfaces,

$$\Omega = \sigma_1 + \lambda\sigma_2 \ , \tag{13}$$

where λ is a constant. Differentiating Eq.(13) w.r.t. 't', we have

$$\dot{\Omega} = \dot{\sigma}_1 + \lambda\dot{\sigma}_2 \ , \tag{14}$$

$$\dot{\Omega} = \varrho_1 x_2 + f_1 + b_1\tau + \Delta + \lambda(\varrho_2 x_4 + f_2 + b_2\tau + \Delta) \ . \tag{15}$$

From Eqs.(4), (8), and (12), we have

$$\dot{\Omega} = (b_1 + \lambda b_2)\tau_{\mathrm{sw}}. \tag{16}$$

In order to derive a control law which switches the system states to the sliding surface $\Omega = 0$, we define a Lyapunov function as:

$$V = \frac{1}{2}\Omega^2 \ . \tag{17}$$

If the derivative $\dot{V}$ is negative definite, then the system is asymptotically stable, i. e., its trajectories will approach the sliding surface, ultimately converging to the origin [26].

$$\dot{V} = \Omega \cdot \dot{\Omega}. \tag{18}$$

To make it negative definite, we define

$$\dot{\Omega} = -\epsilon \cdot \mathrm{sat}(\Omega) \ , \tag{19}$$

where ϵ is a switching gain and sat is the saturation function defined as:

$$\mathrm{sat}(\Omega) = \begin{cases} \mathrm{sgn}(\Omega), & \text{if } |\Omega| \geq 1 \\ \Omega, & \text{if } |\Omega| < 1 \end{cases}$$

and

$$\mathrm{sgn}(\Omega) = \begin{cases} 1, & \text{if } \Omega > 0 \\ -1, & \text{if } \Omega < 0. \end{cases}$$

The switching gain can be selected in two ways: one is the switching gain with a constant value ϵ and the other is the switching gain $\epsilon(x)$ which is a function of the state variables. If the switching gain is selected as a constant, then it must be a positive constant to fulfil the stability condition for the second-level sliding surface. If we choose a state-dependent switching gain, then it can be defined as

$$\epsilon(x) = \beta(\Omega^2 + \gamma),$$

where β and γ are positive constants. Now Eq.(18) becomes

$$\dot{V} = -\epsilon(x) \cdot \Omega \cdot \mathrm{sat}(\Omega) < 0. \tag{20}$$

From Eqs.(16) and (19), the switching control law is obtained as:

$$\tau_{\mathrm{sw}} = \frac{-\epsilon(x) \cdot \mathrm{sat}(\Omega)}{\mid b_1 + \lambda b_2 \mid + \delta} . \tag{21}$$

Finally, total control input is

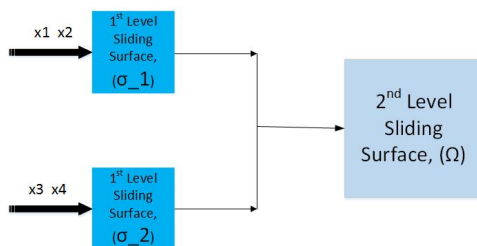$$\tau = \tau_{\mathrm{eq1}} + \tau_{\mathrm{eq2}} + \tau_{\mathrm{sw}} . \tag{22}$$

Fig. 2. Schematic block-diagram of HSMC.

4. DECOUPLED SLIDING MODE CONTROL

Decoupled sliding mode control is a nonlinear control design technique. It is widely used for the stabilization of underactuated nonlinear systems [6, 23, 28]. The basic structural difference between HSMC and DSMC is that in the latter, we use an intermediate variable instead of the second-level sliding surface. DSMC also consists of an equivalent control and a switching control.

The main idea of DSMC is to decouple the RIP system into two subsystems: subsystem I and subsystem II. Subsystem I consists the state variables x_1 and x_2, while the subsystem II includes the state variables x_3 and x_4. The control objective is to drive the states of subsystem I to the unstable equilibrium point at the origin. For this purpose, it is reasonable to consider the information of subsystem II as secondary information. An

intermediate variable ζ is used to accomplish this task as illustrated in Figure 3. Hence sliding surfaces for DSMC are modified as:

$$\sigma_1 = \varrho_1(x_1 - \zeta) + x_2 , \tag{23}$$

$$\sigma_2 = \varrho_2 x_3 + x_4 , \tag{24}$$

where ζ is the decay oscillation [23]. It is defined as:

$$\zeta = \mathrm{sat}\left(\frac{\sigma_2}{\psi}\right) \cdot \varphi , \qquad 0 < \varphi < 1 , \tag{25}$$

where ψ is the boundary layer of σ_2 which is used to smooth the intermediate variable ζ. The final control input of DSMC is derived as:

$$\tau = \tau_{\mathrm{eq}} + \tau_{\mathrm{sw}} , \tag{26}$$

where

$$\tau_{\mathrm{eq}} = \frac{-\varrho_1 x_2 - f_1 - \Delta}{\mid b_1 \mid + \delta} , \tag{27}$$

$$\tau_{\mathrm{sw}} = \frac{-\epsilon \cdot \mathrm{sat}(\sigma_1)}{\mid b_1 \mid + \delta}. \tag{28}$$

The equivalent control τ_{eq} is derived from Eq.(23) and the switching τ_{sw} is derived by defining a Lyapunov function similar to HSMC.
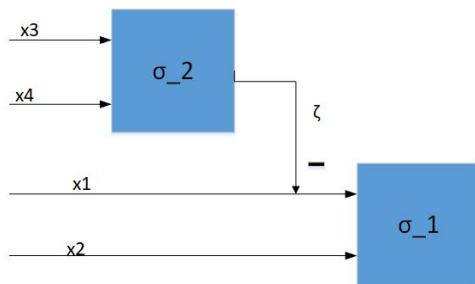

Fig. 3. Structure of DSMC.

5. THEORETICAL STABILITY

This section consists of two theorems which deal with the asymptotic stability of the second-level sliding surface and the first-level sliding surfaces. To prove these theorems, we use Lyapunov stability theory and Barbalat lemma [40].

Theorem 5.1. (Asymptotic Stability of the Second Level Surface) Consider a class of under-actuated dynamical systems of the form (3). If we use the control law (22) along with sliding surfaces as designed in Eqs.(5), (9), and (13), then the second-level sliding surface is asymptotically stable.

P r o o f. Consider the Lyapunov function as defined in Eq.(17),

$$V = \frac{\Omega^2}{2} .$$

Differentiating the above equation w.r.t. 't', we get

$$\dot{V} = \Omega \cdot \dot{\Omega} ,$$
$$\dot{V} = -\epsilon(x) \cdot \Omega \cdot \text{sat}(\Omega) .$$

Integrating both sides of the last equation from 0 to t, we have

$$\int_0^t \dot{V} d\chi = -\int_0^t \epsilon(x) \cdot \Omega \cdot \text{sat}(\Omega) \, d\chi ,$$

$$V(t) - V(0) = -\int_0^t \epsilon(x) \cdot \Omega \cdot \text{sat}(\Omega) \, d\chi ,$$

$$V(0) = V(t) + \int_0^t \epsilon(x) \cdot \Omega \cdot \text{sat}(\Omega) \, d\chi ,$$

$$V(0) \geq \int_0^t \epsilon(x) \cdot \Omega \cdot \text{sat}(\Omega) \, d\chi .$$

The steady state form of the above equation is given by

$$\lim_{t \to \infty} \int_0^t \epsilon(x) \cdot \Omega \cdot \text{sat}(\Omega) \, d\chi \leq V(0) < \infty . \tag{29}$$

According to Barbalat lemma [40],

$$\lim_{t \to \infty} \epsilon(x) \cdot \Omega \cdot \text{sat}(\Omega) = 0 . \tag{30}$$

It follows from Eq.(30) that $\lim_{t \to \infty} \Omega = 0$. As a consequence of this, we can conclude that the second-level sliding surface is asymptotically stable. $\square$

Theorem 5.2. (Asymptotic Stability of the First-Level Surfaces)
Consider an under-actuated dynamical system of the form (3). If control law adopted is as given in (22) with the sliding surfaces as designed in Eqs.(5), (9), and (13), then the first-level sliding surfaces are asymptotically stable.

P r o o f. The proof of this theorem is sketched in the sequel. From Eq.(29) and considering $\dot{V} = \Omega \dot{\Omega} < \infty$, it follows that $\Omega, \dot{\Omega} \in L^\infty$, where L^∞ denotes the space of all bounded functions. From Eqs.(13) and (14), we can see that the linear combination of the first level sliding surfaces σ_i, $i = 1, 2$ and their time derivatives $\dot{\sigma}_i$, $i = 1, 2$ are also bounded functions, i. e., $\sigma_1 + \lambda \sigma_2 \in L^\infty$ and $\dot{\sigma}_1 + \lambda \dot{\sigma}_2 \in L^\infty$. It follows that $\sigma_1, \sigma_2 \in L^\infty$ and $\dot{\sigma}_1, \dot{\sigma}_2 \in L^\infty$. As a consequence of this, we have

$$\sup_{t \geq 0} | \sigma_i | = \| \sigma_i \|_\infty < \infty, \ i = 1, 2.$$

Therefore, the steady state form of the first level surfaces will be as given below

$$\lim_{t\to\infty} \sigma_1 = \lim_{t\to\infty} \sigma_2 = 0.$$

This proves the asymptotic stability of the first level surfaces. □

6. NUMERICAL SIMULATIONS

Two nonlinear controllers HSMC and DSMC, and one linear state feedback controller (Pole Placement) are applied to the RIP system and simulated in MATLAB. The comparative performance is presented in this section. The values of the model parameters and constants used for the simulations are taken from [19]. The values are: $m = 0.125\,\mathrm{kg}$, $L = 0.1675\,\mathrm{m}$, $r = 0.215\,\mathrm{m}$, $\eta_m = 0.87$, $\eta_g = 0.85$, $K_t = 0.00767$, $K_m = 0.00767$, $K_g = 70$, $R_m = 2.6$, $J_m = 0.0035$, $B_{\mathrm{eq}} = 0.004$, $g = 9.8\,\mathrm{m.sec^{-2}}$, $J_{\mathrm{eq}} = 0.0023$. Values of the design parameters of HSMC and DSMC are $\varrho_1 = 5$, $\varrho_2 = 0.98$, $\lambda = -0.481$, $\psi = 22$, $\varphi = 0.9425$, $\delta = 0.0001$, and $\epsilon = 10$.

In Figure 4, we compare HSMC with state-dependent switching gain to HSMC with
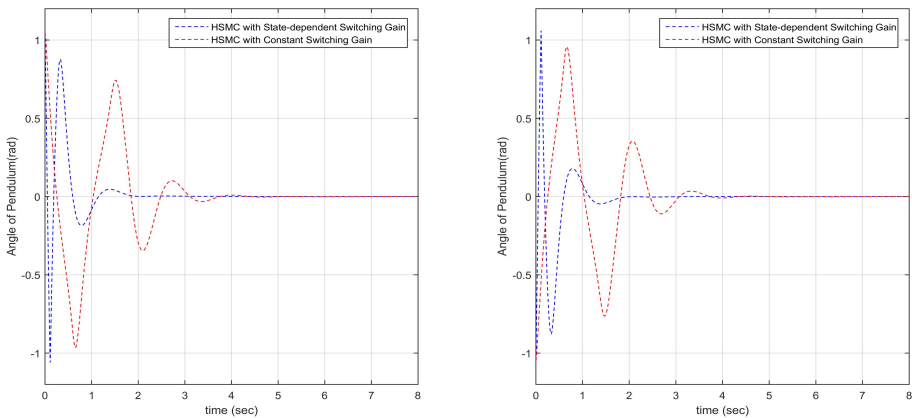
Fig. 4. Variation of angle of the pendulum with time starting from
initial conditions $[\frac{\pi}{3}\,0\,0\,0]^T$ and $[-\frac{\pi}{3}\,0\,0\,0]^T$.

constant switching gain. It can be seen that response time of the proposed HSMC is much faster as compared to the conventional HSMC. Figures 5 and 6 show the comparison of proposed HSMC with DSMC and conventional linear state feedback controller based on pole placement technique. Simulation results demonstrate the stabilization of the RIP system is achieved from proposed HSMC is much quicker and smoother than DSMC and pole placement technique.

We introduce a sinusoidal external disturbance, $\Delta = \sin t$, to test the robustness of our proposed controller and DSMC. The simulation results shown in Figures 7 and 8
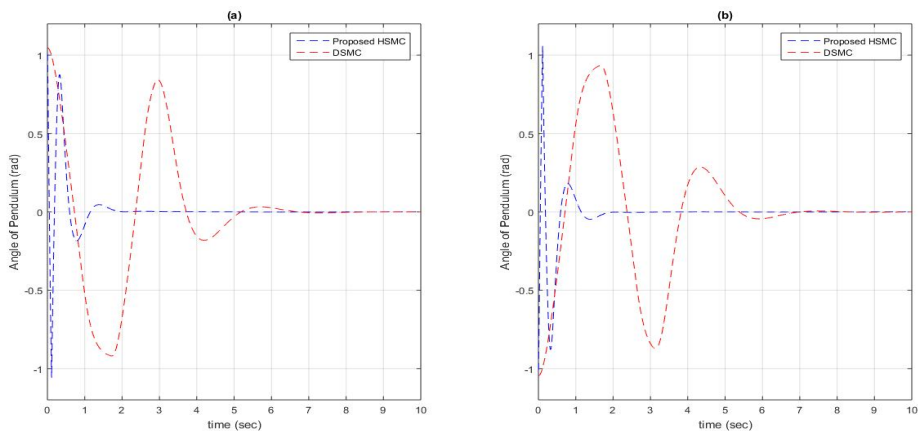
Fig. 5. Comparison of the proposed HSMC and DSMC with Initial Conditions at $[\frac{\pi}{3}\,0\,0\,0]^T$ and $[-\frac{\pi}{3}\,0\,0\,0]^T$.
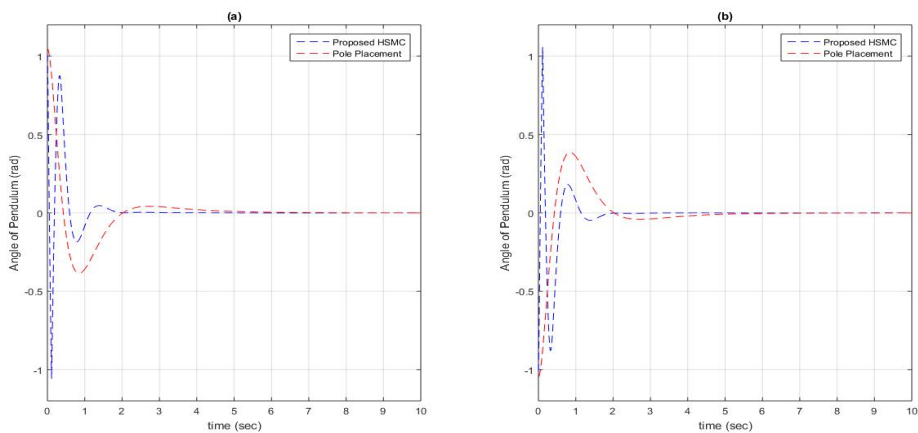

Fig. 6. Comparison of the proposed HSMC and Pole placement technique with initial conditions at $[\frac{\pi}{3}\,0\,0\,0]^T$ and $[-\frac{\pi}{3}\,0\,0\,0]^T$.

demonstrate the stabilization of the RIP system by using these controllers. For these simulations, we fluctuate the external disturbance by varying the amplitude of the sinusoidal disturbance to validate the robustness of the proposed HSMC and DSMC. It can be seen from these figures that our proposed HSMC stabilizes the RIP system much quicker than DSMC in presence of the external disturbances. Further, by keeping the amplitude of the external disturbance fix, we change the values of parameters L, r and m to check controller robustness for parameter uncertainty. The results are shown in

Figures 9 and 10. From these results, it is clear that the proposed controller is robust with parametric uncertainty. DSMC shows oscillations and large response time which is not the desirable performance.
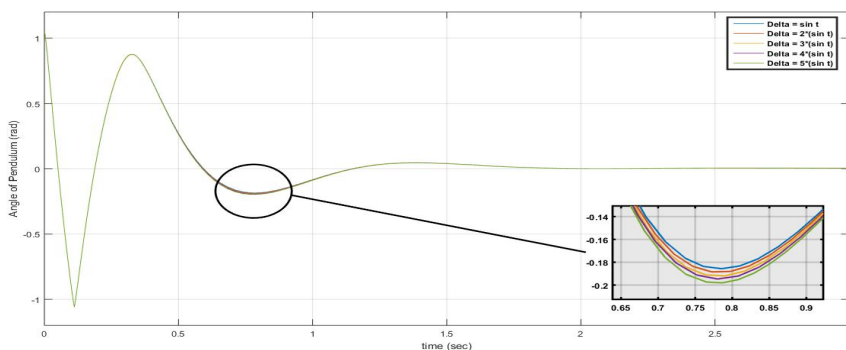

Fig. 7. Robustness test of the proposed HSMC for sinusoidal external disturbances.
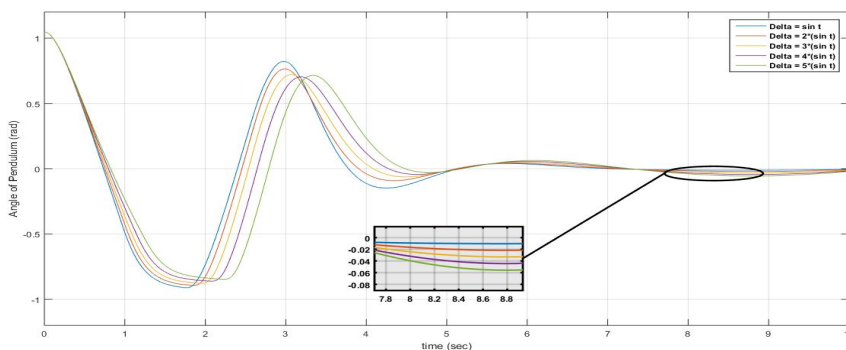

Fig. 8. Robustness test of DSMC for sinusoidal external disturbances.

7. CONCLUSION

In this paper, our study is focused on the potential uses of SMC methods for stabilization of the RIP systems. Two nonlinear controllers HSMC and DSMC are successfully designed for the RIP systems in presence of external disturbances. HSMC for the RIP system consists of two first-level surfaces and one second-level sliding surface. The second-level sliding surface is used to interact the first level sliding surfaces and to obtain switching control. DSMC also consists of two sliding surfaces. In this technique,
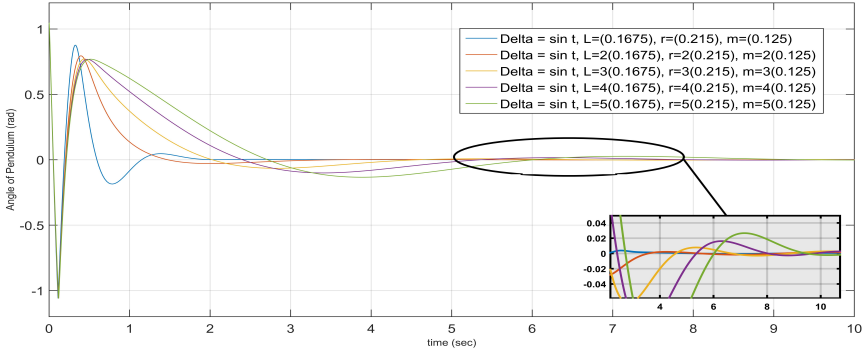
Fig. 9. Variation in system states using the proposed HSMC for
varying values of parameters.
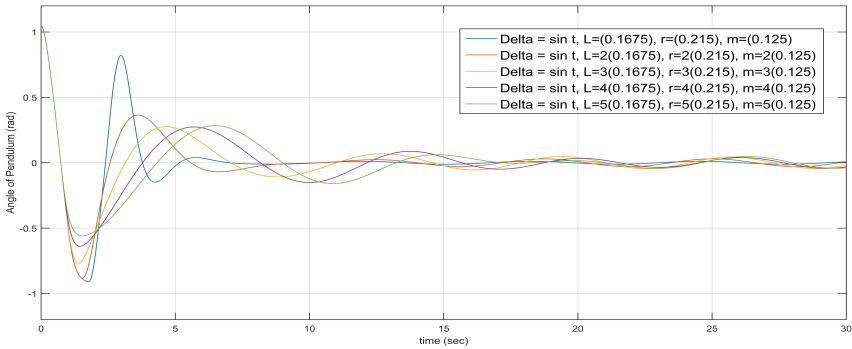
Fig. 10. Variation in system states with DSMC for varying values of
parameters.

an intermediate variable (ζ in this article) is introduced to pass the information of one
sliding surface to the other.

We have proposed a variant of HSMC with a state-dependent switching gain. Detailed
simulations are carried out to show the effectiveness of our proposed controller. Simu-
lations include the comparison of the proposed controller with the conventional HSMC
using a constant switching gain, DSMC, and state feedback controller based on pole
placement technique. Moreover, we have tested the robustness of the proposed HSMC
for variable external disturbances and parameter uncertainties. The proposed HSMC
showed robust stabilization in presence of bounded external disturbances and parameter
variations as compared to DSMC. Further, asymptotic stability of the first-level and the
second-level sliding surfaces of the proposed controller are also proved in this paper.

R E F E R E N C E S

[1] M. E. Antonio-Toledo, E. N. Sanchez, A. Y. Alanis, J. Florez, and M. A. Perez-Cisneros: Real-time integral backstepping with sliding mode control for a quadrotor UAV. IFAC-Papers Online *51* (2018), 549–554. DOI:10.1016/j.ifacol.2018.07.337

[2] Y. A. Butt: Robust stabilization of a class of nonholonomic systems using logical switching and integral sliding mode control. Alexandria Engrg. J. *57* (2018), 1591–1596. DOI:10.1016/j.aej.2017.05.017

[3] G. J. Baker and J. A. Blackburn: The Pendulum: A Case Study in Physics. Oxford University Press, New York 2002.

[4] Y. F. Chen and A. C. Huang: Adaptive control of rotary inverted pendulum system with time-varying uncertainties. Nonlinear Dynamics *76* (2014), 95–102. DOI:10.1007/s11071-013-1112-4

[5] J. J. Choi and J. S. Kim: Robust control for rotational inverted pendulums using output feedback sliding mode controller and disturbance observer. KSME Int. J. *17* (2003), 1466–1474. DOI:10.1007/bf02982326

[6] R. Coban and B. Ata: Decoupled sliding mode control of an inverted pendulum on a cart: An experimental study. In: IEEE International Conference on Advanced Intelligent Mechatronics, Germany 2017. DOI:10.1109/aim.2017.8014148

[7] K. Furuta, M. Yamakita, and S. Kobayashi: Swing-up control of inverted pendulum using pseudo-state feedback. J. Systems Control Engrg. *206* (1992), 263–269. DOI:10.1243/pime_proc_1992_206_341_02

[8] W. Gao and J. C. Hung: Variable structure control of nonlinear systems: A new approach. IEEE Trans. Industr. Electronics *40* (1993), 45–55. DOI:10.1109/41.184820

[9] F. Grasser, A. D′Arrigo, S. Colombi, and A. C. Rufer: Joe: a mobile, inverted pendulum. IEEE Trans. Industr. Electron. *49* (2002), 107–114. DOI:10.1109/41.982254

[10] I. Hassanzadeh and S. Mobayen: Controller design for rotary inverted pendulum system using evolutionary algorithms. Math. Problems Engrg. *2011* (2011), 1–17. DOI:10.1155/2011/572424

[11] J. Irfan, J. Rehan, J. Zhao, J. Rizwan, and S. Abdus: Mathematical model analysis and control algorithms design based on state feedback method of rotary inverted pendulum. Int. J. Research Engrg. Technol. *1* (2013), 41–50.

[12] Z. Jia, J. Yu, Y. Mei, Y. Chen, Y. Shen, and X. Ai: Integral backstepping sliding mode control for quadrotor helicopter under external uncertain disturbances. Aerospace Science Technol. *68* (2017), 299–307. DOI:10.1016/j.ast.2017.05.022

[13] S. Jadlovska and J. Sarnovsky: Modelling of classical and rotary inverted pendulum systems: A generalized approach. J. Electr. Engrg. *64* (2013), 12–19. DOI:10.2478/jee-2013-0002

[14] A. Jose, C. Augustine, S. M. Malola, and K. Chacko: Performance study of PID controller and LQR technique for inverted pendulum. World J. Engrg. Technol. *3* (2015), 76–81. DOI:10.4236/wjet.2015.32008

[15] A. Kchaou, A. Naamane, Y. Koubaa, N. Mʹsirdi: Second order sliding mode-based MPPT control for photovoltaic applications. Solar Energy *155* (2017), 758–769. DOI:10.1016/j.solener.2017.07.007

[16] O. Kaynak, K. Erbatur, and M. Ertugrul: The fusion of computationally intelligent methodologies and sliding mode control-A survey. IEEE Trans. Industr. Electron. *48* (2001), 4–17. DOI:10.1109/41.904539

[17] S. Kurode, A. Chalanga, and B. Bandyopadhyay: Swing-up and stabilization of rotary inverted pendulum using sliding modes. In: Preprints of the 18th IFAC World Congress, Milano 2011. DOI:10.3182/20110828-6-it-1002.02933

[18] M. A. Khanesar, M. Teshnehlab, and M. A. Shoorehdeli: Fuzzy sliding mode control of rotary inverted pendulum. In: Proc. 5th IEEE International Conference on Computational Cybernetics, Tunisia 2007. DOI:10.1109/icccyb.2007.4402019

[19] M. A. Khanesar, M. Teshnehlab, and M. A. Shoorehdeli: Sliding mode control of rotary inverted pendulum. In: Proc. 15th Mediterannean Conference on Control and Automation, Greece 2007. DOI:10.1109/med.2007.4433653

[20] X. Liu, A. N. Vargas, X. Yu, and L. Xu: Stabilizing two-dimensional stochastic systems through sliding mode control. J. Franklin Inst. *354* (2017), 5813–5824. DOI:10.1016/j.jfranklin.2017.07.015

[21] B. Lu, Y. Fang, and N. Sun: Sliding mode control for underactuated overhead cranes suffering from both matched and unmatched disturbances. Mechatronics *47* (2017), 116–125. DOI:10.1016/j.mechatronics.2017.09.006

[22] X. Lin, J. Nie, Y. Jiao, K. Liang, and H. Li: Adaptive fuzzy output feedback stabilization control for the underactuated surface vessel. Appl. Ocean Res. *74* (2018), 40–48. DOI:10.1016/j.apor.2018.01.015

[23] J. C. Lo and Y. H. Kuo: Decoupled fuzzy sliding-mode control. IEEE Trans. Fuzzy Systems *6* (1998), 426–435. DOI:10.1109/91.705510

[24] N. Muskinja and B. Tovornik: Swinging up and stabilization of a real inverted pendulum. IEEE Trans. Industr. Electron. *53* (2006), 631–639. DOI:10.1109/tie.2006.870667

[25] H. Mei and Z. He: Study on stability control for single link rotary inverted pendulum. In: Proc. International Conference on Mechanic Automation and Control Engineering, Wuhan 2010. DOI:10.1109/mace.2010.5536653

[26] Y. J. Mon and C. M. Lin: Hierarchical fuzzy sliding-mode control. In: Proc. IEEE International Conference on Fuzzy Systems, Greece 2002. DOI:10.1109/fuzz.2002.1005070

[27] Q. H. Ngo, N. P. Nguyen, C. N. Nguyen, T. H. Tran, and Q. P. Ha: Fuzzy sliding mode control of an offshore container crane. Ocean Engrg. *140* (2017), 125–134. DOI:10.1016/j.oceaneng.2017.05.019

[28] R. Nagarale and B. Patre: Decoupled neural fuzzy sliding mode control of nonlinear systems. In: IEEE International Conference on Fuzzy Systems, Hyderabad 2013. DOI:10.1109/fuzz-ieee.2013.6622321

[29] S. E. Oltean: Swing-up and stabilization of the rotational inverted pendulum using PD and fuzzy-PD controllers. Procedia Technol. *12* (2014), 57–64. DOI:10.1016/j.protcy.2013.12.456

[30] N. Phuong, H. Loc, and T. Tuan: Control of two wheeled inverted pendulum using sliding mode technique. Int. J. Engrg. Res. Appl. *3* (2013), 1276–1282.

[31] W. Perruquetti and J. P. Barbot: Sliding Mode Control in Engineering. CRC Press, 2002. DOI:10.1201/9780203910856

[32] D. Qian and J. Yi: Hierarchical Sliding Mode Control for Under-actuated Cranes. Springer–Verlag, Berlin 2015. DOI:10.1007/978-3-662-48417-3

[33] M. S. Qureshi, P. Swarnkar, and S. Gupta: A supervisory on-line tuned fuzzy logic based sliding mode control for robotics: An application to surgical robots. Robotics Autonom. Systems *109* (2018), 68–85. DOI:10.1016/j.robot.2018.08.008

[34] D. Qian, J. Yi, and D. Zhao: Hierarchical sliding mode control for a class of simo under-actuated systems. Control Cybernet. *37* (2008), 159–175.

[35] D. Qian, J. Yi, D. Zhao, and Y. Hao: Hierarchical sliding mode control for series double inverted pendulums system. In: Proc. International Conference on Intelligent Robots and Systems, Beijing 2006. DOI:10.1109/iros.2006.282521

[36] Z. Song, K. Sun, and S. Ling: Stabilization and synchronization for a mechanical system via adaptive sliding mode control. ISA Trans. *68* (2017), 353–366. DOI:10.1016/j.isatra.2017.02.013

[37] J. E. Solanes, L. Gracia, P. Munoz-Benavent, J. V. Miro, V. Girbes, and J. Tornero: Human-robot cooperation for robust surface treatment using non-conventional sliding mode control. ISA Trans. *80* (2018), 528–541. DOI:10.1016/j.isatra.2018.05.013

[38] J. J. E. Slotine: Sliding controller design for nonlinear systems. Int. J. Control *40* (1984), 421–434. DOI:10.1080/00207178408933284

[39] V. Sirisha and A. S. Junghare: A comparative study of controllers for stabilizing a rotary inverted pendulum. Int. J. Chaos, Control, Modell. Simul. *3* (2014), 1–13. DOI:10.5121/ijccms.2014.3201

[40] J. J. E. Slotine and W. Li: Applied Nonlinear Control. Prentice Hall International Inc., 1991.

[41] A. Tapia, M. Bernal, and L. Fridman: Nonlinear sliding mode control design: An LMI approach. Systems Control Lett. *104* (2017), 38–44. DOI:10.1016/j.sysconle.2017.03.011

[42] L. A. Tuan, S. G. Lee, L. C. Nho, and H. M. Cuong: Robust controls for ship-mounted container cranes with viscoelastic foundation and flexible hoisting cable. Proc. Inst. Mechan. Engineers, Part I: J. Systems Control Engrg. *229* (2015), 662–674. DOI:10.1177/0959651815573903

[43] L. A. Tuan, H. M. Cuong, S. G. Lee, L. C. Nho, and K. Moon: Nonlinear feedback control of container crane mounted on elastic foundation with the flexibility of suspended cable. J. Vibration Control *22* (2016), 3067–3078. DOI:10.1177/1077546314558499

[44] V. I. Utkin and S. K. Korovin: Application of sliding mode to static optimization. Automatic Remote Control *4* (1972), 570–579.

[45] V. I. Utkin and K. D. Yagn: Methods for construction of discontinuity planes in multidimensional variable structure systems. Automat. Remote Control *39* (1978), 72–77.

[46] V. I. Utkin and K. D. Yagn: Variable structure systems with sliding modes. IEEE Trans. Automat. Control *22* (1997), 212–222. DOI:10.1109/tac.1977.1101446

[47] V. I. Utkin, J. Guldner, and J. Shi: Sliding Mode Control in Electro-Mechanical Systems. CRC Press, 2009. DOI:10.1201/9781420065619

[48] Y. J. Wu and G. F. Li: Adaptive disturbance compensation finite control set optimal control for PMSM systems based on sliding mode extended state observer. Mechan. Systems Signal Process. *98* (2018), 402–414. DOI:10.1016/j.ymssp.2017.05.007

[49] A. Wu, X. Zhang, and Z. Zhang: A control system based on the Lagrange modeling method for a single link rotary inverted pendulum. Engrg. Sci. *7* (2005), 11–15.

[50] J. Wen, Y. Shi, and X. Lu: Stabilizing a rotary inverted pendulum based on logarithmic Lyapunov function. J. Control Science Engrg. *2017* (2017), 1–11. DOI:10.1155/2017/4091302

[51] I. Yigit: Model free sliding mode stabilizing control of a real rotary inverted pendulum. J. Vibration Control *23* (2017), 1645–1662. DOI:10.1177/1077546315598031

[52] M. Yue, C. An, Y. Du, and J. Sun: Indirect adaptive fuzzy control for a nonholonomic/underactuated wheeled inverted pendulum vehicle based on a data-driven trajectory planner. Fuzzy Sets Systems *290* (2016), 158–177. DOI:10.1016/j.fss.2015.08.013

[53] J. Zhang, Q. Zhang, and Y. Wang: A new design of sliding mode control for Markovian jump systems based on stochastic sliding surface. Inform. Sci. *391* (2017), 9–27. DOI:10.1016/j.ins.2017.02.005

[54] Y. Zhao, P. Huang, and F. Zhang: Dynamic modeling and super-twisting sliding mode control for tethered space robot. Acta Astronautica *143* (2018), 310–321. DOI:10.1016/j.actaastro.2017.11.025

Muhammad Idrees, Department of Mathematics and Statistics, The University of Lahore, Sargodha Campus 40100. Pakistan.
   e-mail: midrees.math@gmail.com

Shah Muhammad, Department of Mathematics, Mirpur University of Science and Technology (MUST), Mirpur-10250 (AJK). Pakistan.
   e-mail: shah.maths@must.edu.pk

Saif Ullah, Department of Mathematics, Government College University Lahore, 54000. Pakistan.
   e-mail: dr.saifullah@gcu.edu.pk